



# Sedimentological and weathering signature investigation of claystones from Northern Bida Basin, Central Nigeria

S. A. Adepoju<sup>a,\*</sup>, O. J. Ojo<sup>b</sup>, O. Olaniyan<sup>a</sup>, T. E. Bamidele<sup>a</sup>, I. S Usman<sup>a</sup>

<sup>a</sup>Department of Geology and Mineral Science, Kwara State University, Malete, Kwara State

<sup>b</sup>Department of Geology, Federal University, Oye-Ekiti

## Abstract

This study investigates claystone samples from the northern Bida Basin, northcentral Nigeria, using sedimentological analysis, bulk geochemical techniques (X-ray fluorescence and inductively coupled plasma mass spectrometry), and statistical methods. The research aims to assess the resource potential of the claystone by analyzing mineralogical compositions, weathering indices, and reconstructing depositional environments with emphasis on economic implications. Sedimentological studies identified two sub-facies; the laminated and massive claystones that ranges in color from white, stained-white, and brown to grey, interpreted as suspension-settled deposits of flocculated clay-sized particles within overbank fines of a floodplain. Geochemical analysis of 10 samples from five locations revealed significant SiO<sub>2</sub> (47.58–78.58%), Al<sub>2</sub>O<sub>3</sub> (12.17–34.35%), and Fe<sub>2</sub>O<sub>3</sub> (0.63–7.11%) contents. Comparison with published values suggests suitability for ceramics and paint production, especially after wet-sieving. Statistical visualization highlighted SiO<sub>2</sub> and Al<sub>2</sub>O<sub>3</sub> as dominant oxides. Factor analysis grouped the geochemical data into: (i) F1-F2 (eigenvalues > 1.0), indicating major influence of SiO<sub>2</sub> and Al<sub>2</sub>O<sub>3</sub>; and (ii) F3-F5 (eigenvalues < 1.0), showing minor contributions. Ratios like Ni/Co (1.14–4.00), Cu/Zn (0.42–4.35), U/Th (0.11–0.87), V/Cr (0.04–2.15), and V/(V+Ni) (0.73–0.95) indicate oxic paleodepositional conditions. Provenance indicators such as Al<sub>2</sub>O<sub>3</sub>/TiO<sub>2</sub> (6.77–20.84), Th/Sc (0.60–4.26), La/Sc (1.59–12.66), and chondrite-normalized REE patterns suggest a source from acidic/silicic igneous rocks. High CIA (88.94–99.49), CIW (96.72–99.94), and PIA (80.40–99.03) values indicate intense weathering in the source area, reflecting non-in-situ clay types. In conclusion, the northern Bida Basin claystones show strong potential as raw materials for ceramics, paint, and brick-making industries.

DOI:10.46481/jnsps.2025.2041

**Keywords:** Claystone, Sedimentology, Paleoweathering, Provenance, Raw materials.

## Article History :

Received: 13 March 2024

Received in revised form: 06 March 2025

Accepted for publication: 29 March 2025

Available online: 17 May 2025

© 2025 The Author(s). Published by the [Nigerian Society of Physical Sciences](#) under the terms of the [Creative Commons Attribution 4.0 International license](#). Further distribution of this work must maintain attribution to the author(s) and the published article's title, journal citation, and DOI.

Communicated by: Omosanya Kamaldeen Olakunle

## 1. Introduction

Clay, primarily found near the Earth's surface, consists of finer-grained clay minerals mixed with quartz, carbonates, and metal oxides [1, 2]. These materials have been extensively

studied for their geological significance and diverse industrial applications, including ceramics, pottery, brick manufacturing, construction materials, and environmental engineering. Ekosse [3] explained that clay forms through primary processes, such as hydrothermal activity and residual weathering, or secondary processes involving erosion, transport, and deposition in environments like lacustrine, deltaic, and lagoonal settings. Clay is vital across various fields, including economics, agriculture,

\*Corresponding author Tel. No.: +234-806-233-9819.

Email address: [suraju.adepoju@kwasu.edu.ng](mailto:suraju.adepoju@kwasu.edu.ng) (S. A. Adepoju)

civil engineering, health, and environmental studies [4]. The location of this study is within the northern Bida Basin in the northcentral Nigeria. The Bida basin is a northwest-southeast trending structure with a sediment thickness of approximately 3.5 km [5]. It is bounded by the Sokoto Basin to the northwest and the Benue Trough to the southeast (Figure 1). The basin hosts significant claystones with potential applications as industrial raw materials, however, their suitability for various industries remains underexplored. Investigating sedimentological characteristics and weathering signatures of these claystones is essential for their economic utilization, particularly in the production of tiles, bricks, ceramics, and as raw materials in the paints, paper, chemical, and construction industries.

Early geological investigations of the Bida Basin were documented by Falconer [6] and Jones [7], while subsequent studies by Adeleye [8], Olaniyan and Olabaniyi [9], and Olugbemiro and Nwajide [10] described fluvial environments for its sandstones and conglomerates. Petrographic analysis by Ojo [11] classified the Bida Formation sandstones as mineralogically immature subarkosic facies and interpreted the claystones as non-marine floodplain deposits. Ojo and Akande [12] identified transgressive to shallow marine sedimentation, occasionally incised by fluvial channels, within the Maastrichtian Enagi Formation. Recent studies by Adepoju *et al.* [13, 14] employed petrographic and geochemical approaches to better understand the basin's origin, concluding that the siliciclastic sediments were sourced from stable continental interiors and deposited in an intracratonic setting. Adepoju and Ojo [15] also evaluated the physico-chemical and mineralogical properties of geophagic clays from the northern Bida Basin, finding them suitable for ingestion, with recommended beneficiation to improve quality. Ghafoor *et al.* [16] emphasized the importance of understanding how weathering influences the geochemical properties of claystones to enhance their industrial effectiveness. This study therefore addresses this gap by examining claystone deposits from five selected locations, focusing on the impact of weathering on their sedimentological and chemical properties and evaluating their industrial applications. The objectives are; to (i) analyze the sedimentary processes influencing elemental distribution during claystone deposition using statistical methods, (ii) determine the paleoenvironmental and depositional conditions of claystone formation through geochemical data, and (iii) compare the claystones' geochemical properties with published data to assess their industrial viability. This research supports Nigeria's economic diversification goals by promoting sustainable utilization of claystone resources for industrial development.

## 2. Geological settings of the Bida Basin

On the structural evolution and features, Braide [17] and Whiteman [18] suggested that the Basin was originated with the opening of the Gulf of Guinea during the tectonic evolution of the Benue Trough which began in the late Jurassic to early Cretaceous. Ojo and Ajakaiye [19] employed landsat imageries, borehole logs, with the geophysical data, and submitted that the basin is bounded by linear faults system trending

northwestern-southeastern (NW-SE). Also, an updated gravity studies of Ojo [20] point to a series of central positive anomalies flanked by negative anomalies, similar to the adjacent Benue trough and typical of rift structures. Adeniyi [21], through ground and aeromagnetic studies had outlined the basin configuration as a wrench movement associated with transform fault systems that was resulted in the creation of the basins within and along the entire Benue Trough, and also the adjacent areas such as the Bida basin. Udensi and Osazuwa [22] has also suggested an estimate of 4,700 m as the maximum thickness of the sedimentary successions in the central traverse based on gravity and magnetic surveys.

The stratigraphy and sedimentation of the Campanian-Maastrichtian successions in the Bida Basin have been documented by several workers (e.g. [7, 9, 23]). For example, Adeleye [23] differentiated Bida Basin geographically into two-folds based on the recognizable and mappable stratigraphic units as the northern Bida sub-Basin, and the southern Bida sub-Basin (Figure 2). In the northern part, the basal Bida Formation (comprising the Doko and Jima members) have Lokoja Formation as its lateral equivalent in the southern part [24]. This formation consists mainly of very poorly sorted pebbly arkose, subarkose and quartzose sandstones, and thought to have been deposited in a braided alluvial fan setting based on the submission, while the latter is dominated by cross-stratified quartzose sandstones, siltstones and claystones. Adeleye and Dessauvage [25] used evidence of leaf impression to assign late Cretaceous age (Campanian–Maastrichtian) for the Bida Formation. The overlying Sakpe Formation on the Bida Formation, comprises mainly of oolitic and pisolitic ironstones with sandy-claystones found locally at the base, and then followed by dominantly oolitic ironstone which exhibits rapid facies changes across the basin [24]. The Enagi Formation overlies the Sakpe Formation, and it was described by Adeleye [25] to be comprises of siltstone with subordinate amounts of sandstones, siltstone-sandstone admixtures and claystone which correlates with the Patti Formation in the southern Bida sub-Basin. Other lithofacies that can also be found include sandstone–siltstone intercalation and claystone. Maastrichtian age is assigned by Adeleye [25] because of its stratigraphic position between the Sakpe ironstone and Batati ironstone. The Batati Formation is the youngest Cretaceous unit in the northern part of the Basin, and it is laterally correlated with the Agbaja Formation in the southern Bida Basin. It consists of argillaceous, oolitic and goethitic ironstones with ferruginous claystone and siltstone intercalations and shaly beds occurring in minor proportions, some of which have yielded nearshore shallow marine to fresh water fauna [25].

## 3. Methodology

The fieldwork was conducted at five locations (Share-SHA; Tshonga-TSH; Kutigi-KUT; Shegba-SHE; and Doko-DOK) within the northern Bida Basin, where lithological descriptions of vertical profiles were created (Figures 3a and 3b). The study area was mapped using equipment such as topographic maps,

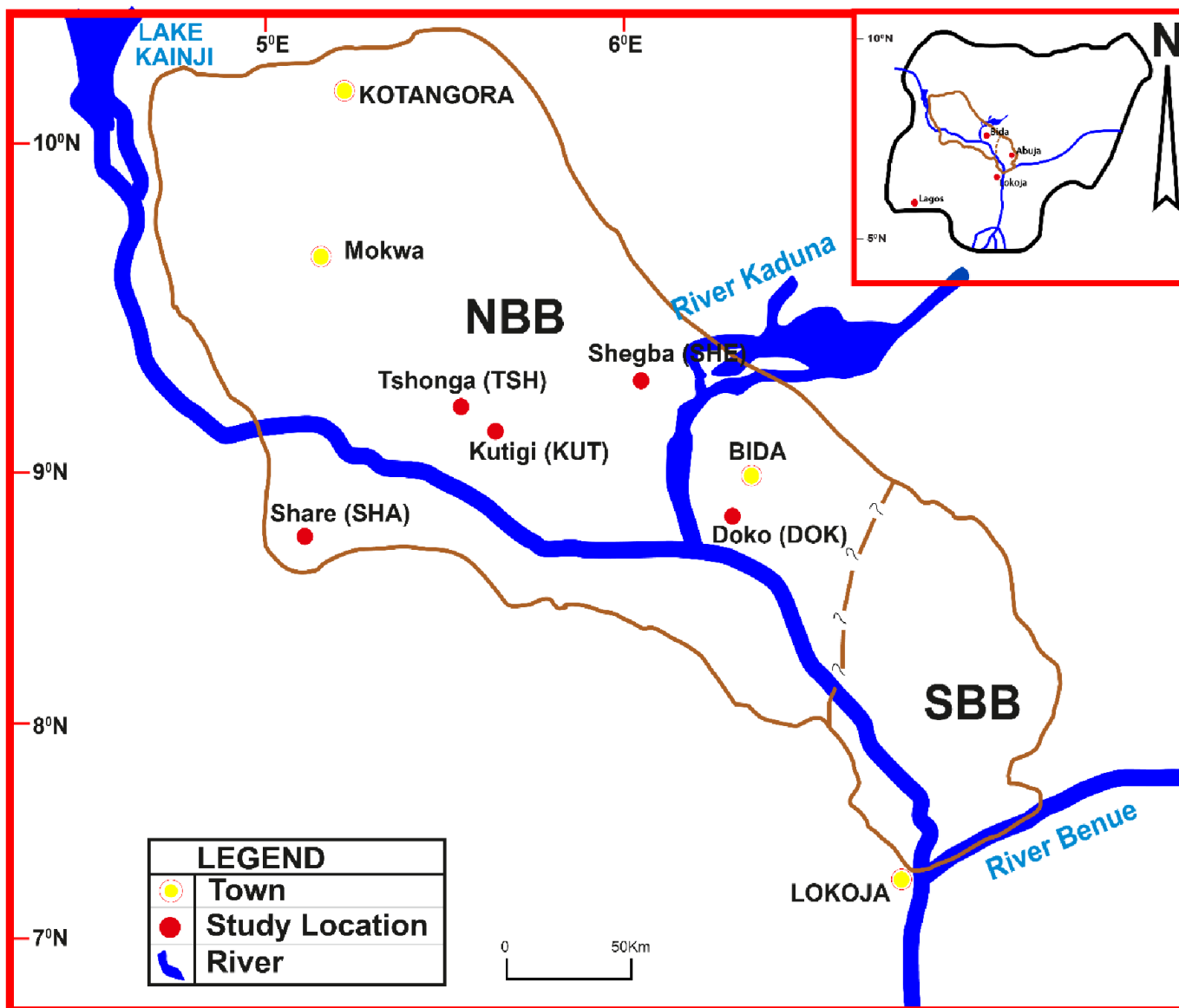


Figure 1. Geological map of Nigeria showing the position of northern Bida Basin, as the area covered for this study.

GPS, clinometer compass, geologic hammer, chisel, measuring tape, digital camera, field notes, hand lens, marker, and sample bags. At each location, the lithological sections were analyzed by measuring bed thickness and identifying textures, colors, and sample distribution. Photographs of outcrops and notable structures were taken for reference.

Ten (10) representative claystone samples (SHA-1 & SHA-1; TSH-1 & TSH-2; KUT-1 & KUT-2, SHE-1 & SHE-2, and DOK-1 & DOK-2) were selected for geochemical analysis at MS Analytical, Canada (Figure 4). A 50–100 g portion of each sample was crushed and pulverized using a mortar and agate tool. Major oxides were analyzed via X-ray fluorescence (XRF), while trace and rare earth elements were analyzed through total digestion (fusion followed by HF+HNO<sub>3</sub> digestion) using Laser Ablation Multicollector Inductively Coupled Plasma Mass Spectrometry (LAM-MC-ICPMS). The resulting

geochemical data were further processed with multivariate statistical methods, including Factor Analysis and Principal Component Analysis, using SPSS software, to gain insights into the environmental factors influencing the sedimentary packages.

#### 4. Field result and dataset presentations

##### 4.1. Lithological description and field data interpretations

The studied claystones were described and classified into facies using standard Miall [26] classification scheme as follows: (i) finely laminated claystone (Fl) and (ii) massive claystone (Fm). These sub-facies exhibit color variations from whitish, brownish, to greyish, with thicknesses ranging from 2.0 to 10.0 m. They are arranged in distinct cycles and exhibit sharp, planar boundaries within each bed unit (Figures 3a and b). Both Fl and Fm sub-facies show evidence of deposition

PERIOD	AGE	NORTHERN BIDA BASIN		SOUTHERN BIDA BASIN		DEPOSITIONAL ENVIRONMENT
<b>UPPER CRETACEOUS</b>	<b>MAASTRICHTIAN</b>	Batati Formation		Agbaja Formation		Continental-Shallow marine
		Enagi Formation		Patti Formation		
		Sakpe Formation				
	<b>CAMPANIAN</b>	Bida Formation	Jima Member	Lokoja Formation	Claystone (member)	Continental Fluvial Deposits
			Doko Member		Sandstone (member)	
				Basal Conglomerate (member)		
<b>PRE-CAMBRIAN</b>	<b>LOWER PROTEROZOIC</b>					Unconformity
						Basement Complex

Figure 2. General stratigraphic framework of the Bida Basin (Modified after Akande *et al.* [29]).

from suspension settling of silt- and clay-sized particles, and they were likely flocculated in overbank and floodplain environments. As noted by Rhee *et al.* [27], preserved lithological successions observed within the study area are interpreted as overbank deposits, with evidence of extensive sheet-like splays formed during large flood events.

#### 4.2. Geochemical datasets

The bulk geochemical datasets, including major oxides, variables, as well as trace and rare earth elements, analyzed from selected studied samples are comprehensively presented in Tables 1 to 3. These tables offer a detailed overview of the composition and characteristics of the studied samples, enabling further analysis and interpretation of the geochemical processes involved. The values of the major oxides ( $\text{SiO}_2$ ;  $\text{Al}_2\text{O}_3$ ;  $\text{Fe}_2\text{O}_3$ ;  $\text{CaO}$ ;  $\text{MgO}$ ;  $\text{Na}_2\text{O}$ ; and  $\text{K}_2\text{O}$ ) are critical for understanding the fundamental chemical composition of the samples. The calculated weathering indices (WI), which reflect the

degree of chemical alteration that has occurred in the claystones are also provided. These indices are critical in evaluating the extent to which the parent material has been weathered or modified by external factors. The inclusion of WI allows for a more comprehensive assessment of the geochemical evolution of the samples and their suitability for specific applications.

Further, the trace elements, especially those that play important roles in geological processes, are detailed in the Table 2. These elements offer valuable information on the geochemical history of the studied claystone samples. Their concentrations can be used to trace specific geological events, such as the formation of certain types of minerals or the influence of particular geochemical environments. The rare earth elements (REEs) are also presented in Table 3. The distribution and concentration of these elements in the analyzed samples provide further insight into the geological processes that led to their enrichment or depletion.

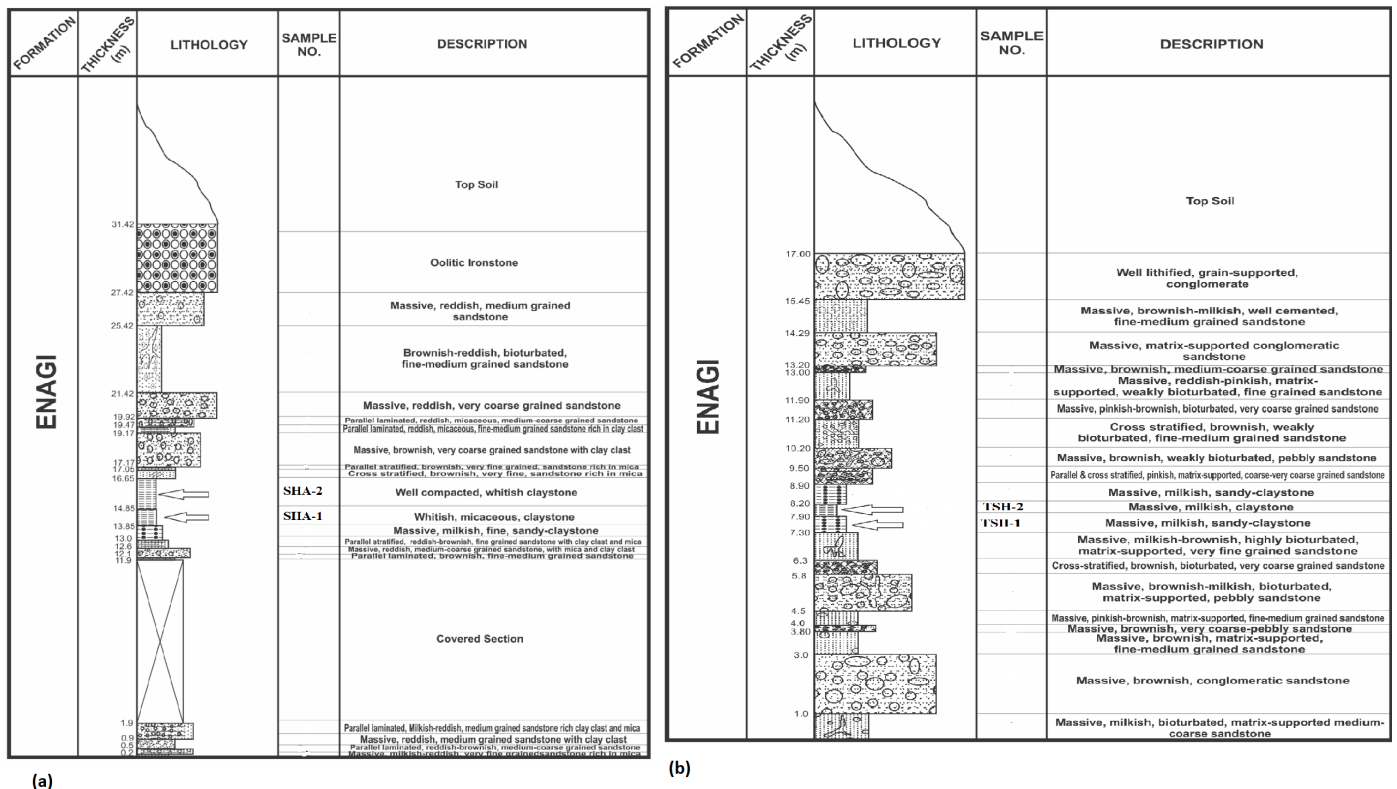


Figure 3. (a) Lithological log of exposed section at Share (SHA) with arrow showing the position of sample collection (Longitude: 004°58'26.9"E; Latitude: 08°49'30.3"N) (b) Lithological log of exposed section at Tshonga (TSH); with arrow showing the position of sample collection (Longitude: 005°08'50.1"E; Latitude: 09°01'27.4"N).

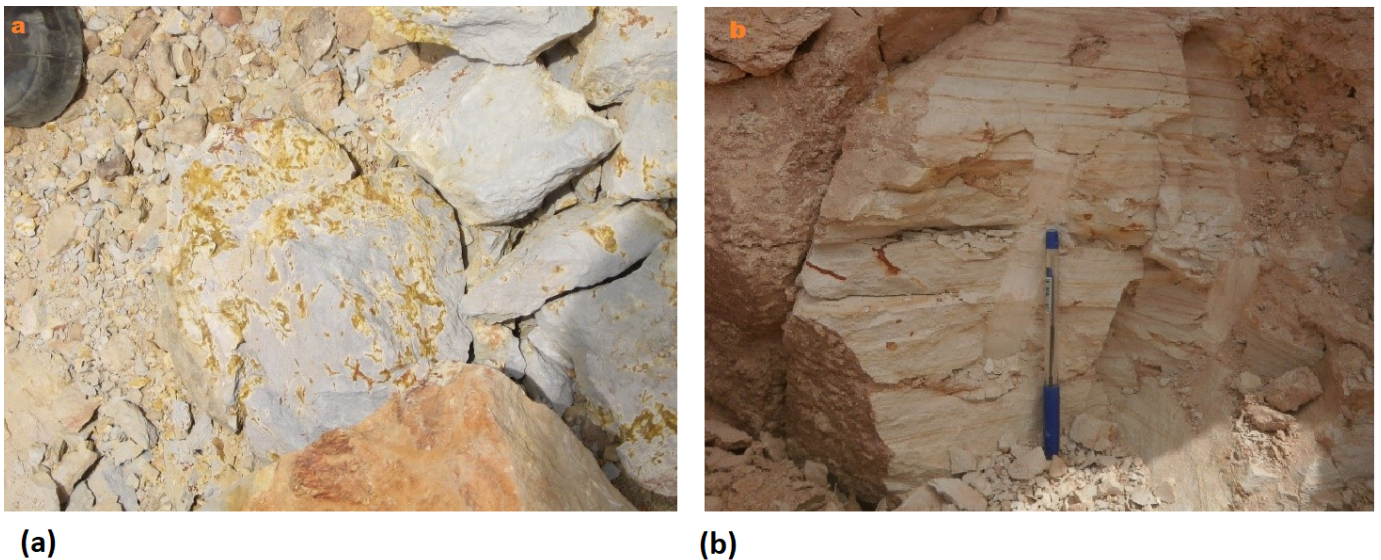


Figure 4. Field photograph showing; (a) grey massive claystone (Fm) sub-facies from exposed section at Tsonga, and (b) whitish laminated claystone (Fl) sub-facies exposed at Kutigi, Share, Tshonga, Shegba and Doko.

Chemical Index of Alteration (CIA) = 
$$\frac{Al_2O_3}{(Al_2O_3 + CaO + Na_2O + K_2O)} \times 100$$
 (After Nesbitt and Young 1982). (1)

Chemical Index of Weathering (CIW) = 
$$\frac{Al_2O_3}{(Al_2O_3 + CaO + Na_2O)} \times 100$$
 (After Harnois, 1988). (2)

Table 1. Major oxides compositions of the studied samples.

Sample Code	SiO <sub>2</sub>	Al <sub>2</sub> O <sub>3</sub>	Fe <sub>2</sub> O <sub>3</sub>	CaO	MgO	Na <sub>2</sub> O	K <sub>2</sub> O	MnO	TiO <sub>2</sub>	P <sub>2</sub> O <sub>5</sub>
DOK-1	78.58	12.17	1.98	0.25	0.18	0.16	0.94	0.01	0.72	0.02
DOK-2	47.58	32.92	2.17	0.01	0.04	0.01	0.15	0.01	1.58	0.06
KUT-1	48.14	34.35	1.85	0.05	0.08	0.01	0.57	0.01	1.95	0.04
KUT-2	64.65	22.65	1.34	0.09	0.06	0.01	0.36	0.01	1.67	0.05
SHE-1	57.98	18.70	7.11	0.30	0.66	0.23	1.74	0.08	0.97	0.03
SHE-2	59.80	18.33	6.98	0.30	0.64	0.22	1.76	0.06	0.96	0.03
SHR-1	54.85	30.34	0.78	0.02	0.07	0.01	0.52	0.01	1.74	0.07
SHR-2	51.94	32.46	0.63	0.02	0.06	0.01	0.37	0.01	1.84	0.06
TSH-1	76.94	12.46	1.63	0.03	0.06	0.01	0.37	0.01	1.84	0.06
TSH-2	54.85	30.34	3.78	0.12	0.07	0.01	0.52	0.01	1.74	0.07
PAAS	62.80	18.90	4.52	1.30	2.20	1.20	3.70	0.11	1.00	0.16
UCC	66.60	14.40	4.04	3.59	2.48	3.27	2.80	0.10	0.64	0.15

Table 2. Major oxides variables, and Weathering Indices (WI) values of the studied samples.

Sample Code	Al <sub>2</sub> O <sub>3</sub> /SiO <sub>2</sub>	Fe <sub>2</sub> O <sub>3</sub> +MgO	K <sub>2</sub> O+Na <sub>2</sub> O	SiO <sub>2</sub> /Al <sub>2</sub> O <sub>3</sub>	Al <sub>2</sub> O <sub>3</sub> /TiO <sub>2</sub>	K <sub>2</sub> O/Al <sub>2</sub> O <sub>3</sub>	CIA	CIW	PIA
DOK-1	0.69	2.21	0.16	1.45	20.84	0.00	99.49	99.94	99.03
DOK-2	0.15	2.16	1.10	6.46	16.86	0.08	90.01	96.72	83.07
KUT-1	0.71	1.93	0.58	1.40	17.62	0.02	98.20	99.83	96.57
KUT-2	0.35	1.40	0.37	2.85	13.56	0.02	98.01	99.56	96.45
SHE-1	0.32	7.77	1.97	3.10	19.34	0.09	89.18	97.24	80.88
SHE-2	0.31	7.62	1.98	3.26	19.05	0.10	88.94	97.24	80.40
SHR-1	0.55	0.85	0.53	1.81	17.44	0.02	98.22	99.90	96.54
SHR-2	0.62	0.69	0.38	1.60	17.64	0.01	98.78	99.91	97.66
TSH-1	0.16	1.69	0.38	6.17	6.77	0.03	96.81	99.68	93.94
TSH-2	0.55	3.85	0.53	1.81	17.44	0.02	97.90	99.57	96.22
PAAS	0.30	6.72	4.90	3.32	18.90	0.20	75.30	88.32	60.56
UCC	0.22	6.52	6.07	4.63	22.50	0.19	59.85	67.73	48.21

Plagioclase Index of Alteration (PIA) =

$$(Al_2O_3 - K_2O)/(Al_2O_3 + CaO + Na_2O - K_2O) \times 100$$

(after Fedo *et al.*, 1995). (3)

#### 4.3. Statistical analysis (Factor analysis and principal component analysis)

The raw geochemical datasets of the analyzed samples were primarily subjected to Principal Component Analysis (PCA) to identify elemental associations and explain the variance within the data sets. Several previous studies (e.g. Reimann *et al.* [28], Pearce *et al.* [29], Svendsen *et al.* [30], Pe-Piper *et al.* [31], and Filzmoser *et al.* [32]) have emphasized the effectiveness of multidimensional data analysis, including PCA, in determining element associations and uncovering hidden patterns. PCA is a widely used multivariate statistical method, particularly suited for geochemical data analysis, as it identifies underlying factors that explain correlations among variables and reduces data dimensionality while retaining key variations.

The major oxide composition PCA Eigen plot for the studied claystone reveals similarities in compositions (Figure 5).

Though, two major elemental associations (F1-F2) were identified as significant in relation to geological processes. The Scree plot which corroborates above deductions on the relationship between the Eigenvalue and cumulative variability, is also presented in Figure 5. Detail explanation on the relations among the factors are presented below.

Factors F1-F2: Factor 1 (F1) explained 71.985% of the total variance (Table 4), with a high loading of 7.199 (greater than 0.75), indicating significant contributions from multiple geological processes, with weathering being the dominant factor. Factor 2 (F2) also showed high loadings (1.875 eigenvalue, >0.75) and explained a cumulative variance of 90.734% (Table 4), reinforcing the dominance of the weathering process. The major oxides linked to weathering, as identified by F1 and F2, include SiO<sub>2</sub> and Al<sub>2</sub>O<sub>3</sub>.

Factors F3-F9: Factors F3 through F9, with eigenvalues below 0.75 (ranging from 0.521 to 0.002), indicate minimal contributions from other major oxides (Fe<sub>2</sub>O<sub>3</sub>, CaO, MgO, Na<sub>2</sub>O, K<sub>2</sub>O, MnO, TiO<sub>2</sub>, and P<sub>2</sub>O<sub>5</sub>) during sediment formation.

Table 3. Trace element compositions (ppm) and ratios of the studied samples.

Sample Code	DOK-1	DOK-2	KUT-1	KUT-2	SHE-1	SHE-2	SHR-1	SHR-2	TSH-1	TSH-2
Cu	11.90	10.34	2.76	3.30	30.00	30.00	1.22	0.87	0.87	1.22
Zn	12.00	24.89	2.50	2.30	60.00	60.00	1.00	0.20	0.20	1.00
Ni	7.50	6.62	1.60	2.30	30.00	30.00	0.30	0.40	0.40	0.30
Co	6.60	4.87	0.60	0.70	16.00	14.00	0.10	0.10	0.10	0.10
U	9.06	2.11	1.91	2.28	5.70	5.60	1.00	0.90	0.90	1.00
Th	39.32	2.44	9.70	20.00	17.60	18.60	1.80	2.10	2.10	1.80
Sr	38.60	21.04	3.20	4.70	71.00	75.00	3.00	1.60	1.60	3.00
V	135.00	17.61	30.00	23.00	116.00	111.00	5.00	5.00	5.00	5.00
Cr	188.00	460.70	22.00	10.70	90.00	120.00	5.30	6.60	66.00	53.00
Ba	121.50	199.70	11.80	12.20	479.00	451.00	8.00	7.40	7.40	8.00
Sc	15.20	3.24	3.50	4.70	15.00	15.00	3.00	2.80	2.80	3.00
Rb	7.20	16.11	1.90	1.20	107.00	108.00	0.80	0.20	0.20	0.80
Zr	115.00	121.80	5.40	8.60	459.00	485.00	3.20	4.50	4.50	3.20
La	162.00	5.15	44.30	16.60	62.40	62.60	19.80	20.40	20.40	19.80
Ni/Co	1.14	1.36	2.67	3.29	1.88	2.14	3.00	4.00	4.00	3.00
Cu/Zn	0.99	0.42	1.10	1.43	0.50	0.50	1.22	4.35	4.35	1.22
U/Th	0.23	0.87	0.20	0.11	0.32	0.30	0.56	0.43	0.43	0.56
V/Cr	0.72	0.04	1.36	2.15	1.29	0.93	0.94	0.76	0.08	0.09
V/(V+Ni)	0.95	0.73	0.95	0.91	0.79	0.79	0.94	0.93	0.93	0.94
Rb/Sr	0.19	0.77	0.59	0.26	1.51	1.44	0.27	0.13	0.13	0.27
Sr/Ba	0.32	0.11	0.27	0.39	0.15	0.17	0.38	0.22	0.22	0.38
Sr/Cu	3.24	2.03	1.16	1.42	2.37	2.50	2.46	1.84	1.84	2.46
La/Sc	10.66	1.59	12.66	3.53	4.16	4.17	6.60	7.29	7.29	6.60

Table 4. Rare Earth Element compositions of the studied samples.

Sample Code	DOK-1	DOK-2	KUT-1	KUT-2	SHE-1	SHE-2	SHR-1	SHR-2	TSH-1	TSH-2
La	162.00	5.15	44.30	16.60	62.40	62.60	19.80	20.40	20.40	19.80
Ce	200.90	13.37	78.70	21.70	131.00	115.00	27.30	27.90	27.90	27.30
Pr	23.97	1.78	8.07	2.82	12.90	13.00	6.60	6.65	6.65	6.60
Nd	77.40	7.41	33.39	10.26	46.70	48.40	26.98	26.66	26.66	26.98
Sm	10.45	1.69	5.10	1.21	9.00	9.20	5.45	4.83	4.83	5.45
Eu	1.83	0.42	0.91	0.30	1.62	1.75	1.13	1.01	1.01	1.13
Gd	9.30	1.70	3.55	1.13	6.90	7.40	4.86	4.74	4.74	4.86
Tb	1.33	0.28	0.41	0.12	1.10	1.10	0.88	0.69	0.69	0.88
Dy	7.14	1.62	2.45	0.86	6.60	6.70	3.53	3.16	3.16	3.53
Ho	1.64	0.33	0.41	0.12	1.13	1.30	0.70	0.57	0.57	0.70
Er	4.58	0.90	1.17	0.36	3.80	4.00	1.70	1.52	1.52	1.70
Tm	0.60	0.08	0.15	0.04	0.58	0.59	0.23	0.19	0.19	0.23
Yb	3.75	0.93	0.99	0.31	3.50	3.90	1.26	1.06	1.06	1.26
Lu	0.55	0.13	0.12	0.03	0.54	0.57	0.17	0.14	0.25	0.25
Total REE	505.44	35.78	179.72	55.86	287.77	275.51	100.59	99.52	99.63	100.67
∑LREE	474.72	29.40	169.56	52.59	262.00	248.20	86.13	86.44	86.44	86.13
∑HREE	28.89	5.97	9.25	2.97	24.15	25.56	13.33	12.07	12.18	13.41
∑LREE/∑HREE	16.43	4.93	18.33	17.71	10.85	9.71	6.46	7.16	7.10	6.42
Eu/Eu*	0.57	0.75	0.65	0.78	0.63	0.65	0.67	0.65	0.65	0.67
La/Lu	30.60	4.00	38.31	57.58	12.00	11.41	12.10	15.13	8.48	8.23
La/Yb	29.13	3.73	30.15	36.18	12.02	10.82	10.59	12.98	12.98	10.59

## 5. Discussions

### 5.1. Paleodepositional conditions and provenance

In provenance studies, elemental distribution in clastic sedimentary rocks, including claystone, is primarily controlled by

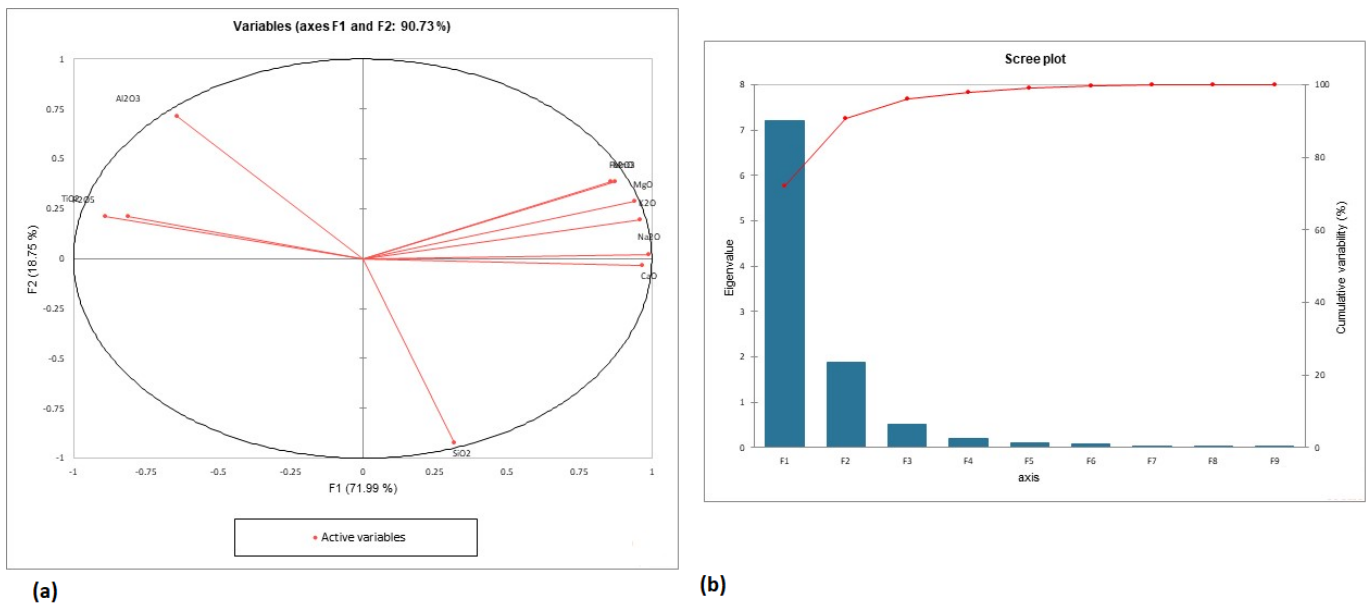


Figure 5. Field photograph showing; (a) Eigenvector plots from the Principal Component Analysis showing SiO<sub>2</sub> and Al<sub>2</sub>O<sub>3</sub> as the major contributors during geological process (b) Scree plot of major oxides showing F1-F2 as significant contributions whereas F3-F9 have minimal contributions.

Table 5. Factor loading and corresponding Principal Component Analysis values of Major oxides.

Factor Loadings	F1	F2	F3	F4	F5	F6	F7	F8	F9
Eigenvalue	7.199	1.875	0.521	0.199	0.112	0.067	0.021	0.004	0.002
Variability (%)	71.985	18.749	5.214	1.994	1.125	0.670	0.205	0.040	0.018
Cumulative %	71.985	90.734	95.948	97.942	99.067	99.737	99.942	99.982	100.000

Table 6. Range of trace elemental ratios for the studied sediments compare with the ratios in similar fractions derived from <sup>1,2</sup>Felsic and Mafic rocks [44], <sup>3</sup>PAAS [45] and <sup>4</sup>UCC [45].

Element Ratio	Average values in Studied Sediments	Published range of values for sediments			
		1	2	3	4
Th/Sc	0.60-4.26	0.84 - 20.50	0.05 - 0.22	0.90	0.79
Th/Co	0.50-28.57	0.67 - 19.40	0.04 - 1.40	0.63	0.63
Th/Cr	0.01-1.87	0.13 - 2.70	0.018 - 0.046	0.13	0.13
La/Sc	1.59-12.66	2.50 - 16.30	0.43 - 0.86	2.40	2.21

geological processes [33], and their geochemical signatures provide valuable insights into the influence of provenance on the depositional system. Several plots from the major oxides to trace with rare earth elements and their ratios, have been widely used to unravel provenance and paleotectonic settings in various geological contexts (e.g., Bhatia [34], Roser and Korsch [35], Kroonenberg [36], Condie [37], Bracciali *et al.* [38]). Also, some sensitive trace elements (e.g., U, Th, Cu, Zn, Ni, Co, V, and Cr) and their ratios are commonly used geochemical indicators to better understand the paleoredox conditions of sediments during deposition [39]. For example, Nath *et al.* [40] suggested that U/Th ratio less than 0.75 indicates oxic conditions, values between 0.75 and 1.25 suggest dyoxic conditions, and ratios greater than 1.25 reflect suboxic to anoxic conditions. Jones and Manning [41] proposed that Ni/Co values below 5.0

represent oxic conditions, values between 5.0 and 7.0 indicate dyoxic conditions, and values above 7.0 are associated with anoxic conditions. Additionally, Deng and Qian [42] found that low Cu/Zn and V/Cr values correspond to oxic conditions, while higher values are indicative of anoxic conditions. Wang [43] further identified that a V/(V+Ni) ratio above 0.84 signals euxinic conditions, values between 0.54 and 0.84 correspond to anoxic conditions, and ratios below 0.46 reflect oxic or dyoxic conditions. In this study, paleodepositional indicators such as Ni/Co (1.14-4.00), Cu/Zn (0.42-4.35), U/Th (0.11-0.87), V/Cr (0.04-2.15), and V/(V+Ni) (0.73-0.95) all indicate oxic paleodepositional conditions for the studied sediments.

In this study, the average values of some provenance indicators in the studied samples (Tables 1-3), such as Al<sub>2</sub>O<sub>3</sub>/TiO<sub>2</sub> (6.77-20.84), Th/Sc (0.60-4.26), Th/Cr (0.01-1.87), La/Sc

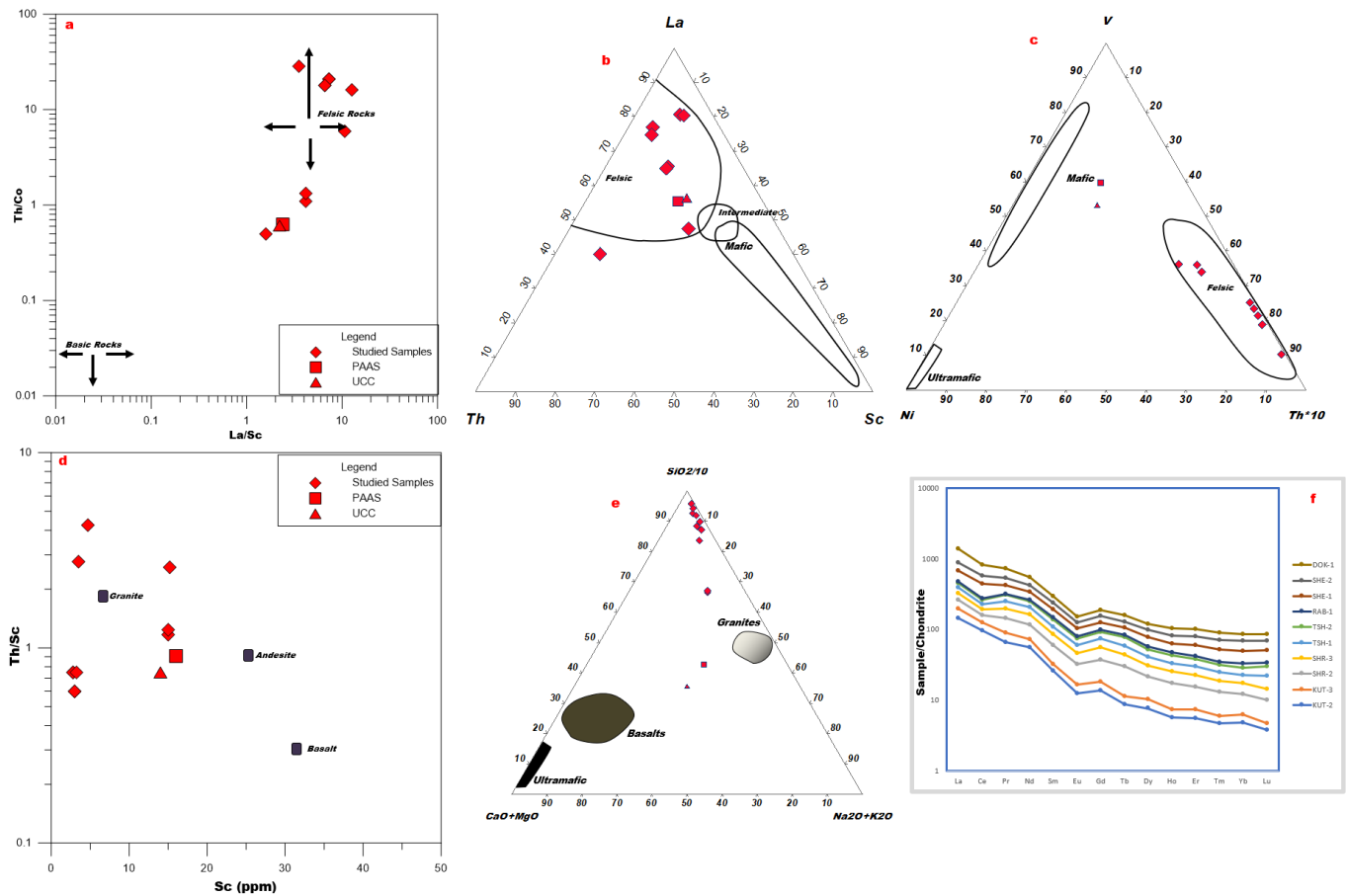


Figure 6. (a) Bivariate provenance plot of Th/Co versus La/Sc after [44], (b & c) Ternary provenance plots of La-Th-Sc after [38] and V-Ni-Th\*10 after [38] showing Felsic fields as the source for the studied claystones; (e & f) bivariate provenance plot of Th/Sc versus Sc after [46] and ternary provenance plot of SiO<sub>2</sub>/10-CaO+MgO-Na<sub>2</sub>O+K<sub>2</sub>O after [45] showing granites fields as the source for the studied claystones, and (f) chondrite-normalized web diagram each rare earth elements in the study claystones showing similar characteristics.

Table 7. Comparison of average values of major oxide composition in the studied claystone with other published data.

Oxides (%)	Present Study	1	2	3	4
SiO <sub>2</sub>	59.53	45.90-48.50	51.70	67.50	68.48
Al <sub>2</sub> O <sub>3</sub>	24.47	33.50-36.10	25.44	26.50	14.94
Fe <sub>2</sub> O <sub>3</sub>	2.83	0.30-0.60	0.5-1.20	0.5-1.20	8.96
MnO	0.01	0.00	ND	0.30	0.00
MgO	0.19	0.00	0.2-0.70	0.10-0.19	1.14
CaO	0.12	0.0-0.50	0.1-0.20	0.18-0.30	1.62
Na <sub>2</sub> O	0.07	0.0-1.6	0.8-3.50	0.20-1.50	0.03
K <sub>2</sub> O	0.73	0.0-1.6	0.00	0.20-1.50	2.05
TiO <sub>2</sub>	0.75	0.0-1.70	1.0-2.80	0.10-1.0	0.00
P <sub>2</sub> O <sub>5</sub>	0.05	0.00	0.00	0.00	0.00
LOI	9.45	0.00	0.00	0.00	0.00

NB: (1) Paper [52], (2) Refractory Bricks [53], (3) Ceramics [54], and (4) Refractory bricks and Ceramics [54].

(1.59-12.66), Eu/Eu\* (0.57-0.78), and (La/Lu)<sub>C<sub>N</sub></sub> (4.00-57.58), are similar to the Post-Archean Australian Shale [44] and Upper Continental Crust [45], therefore, suggesting an igneous rock source (Table 5). Also, the bivariate plot of Th/Co versus La/Sc (Figure 6a) after Cullers [44], and ternary plots of La-Th-Sc and

V-Ni-Th\*10 (Figures 6b & c) after Bracciali *et al.* [38], point to a felsic source rock. In addition, the Th/Sc versus Sc plot (Figure 6d) after Condie and Wronkiewicz [46], and ternary plots of SiO<sub>2</sub>/10-(CaO+MgO)-(Na<sub>2</sub>O+K<sub>2</sub>O) (Figure 6e) after Taylor and McLennan [45], indicate granitic rocks as a potential prove-

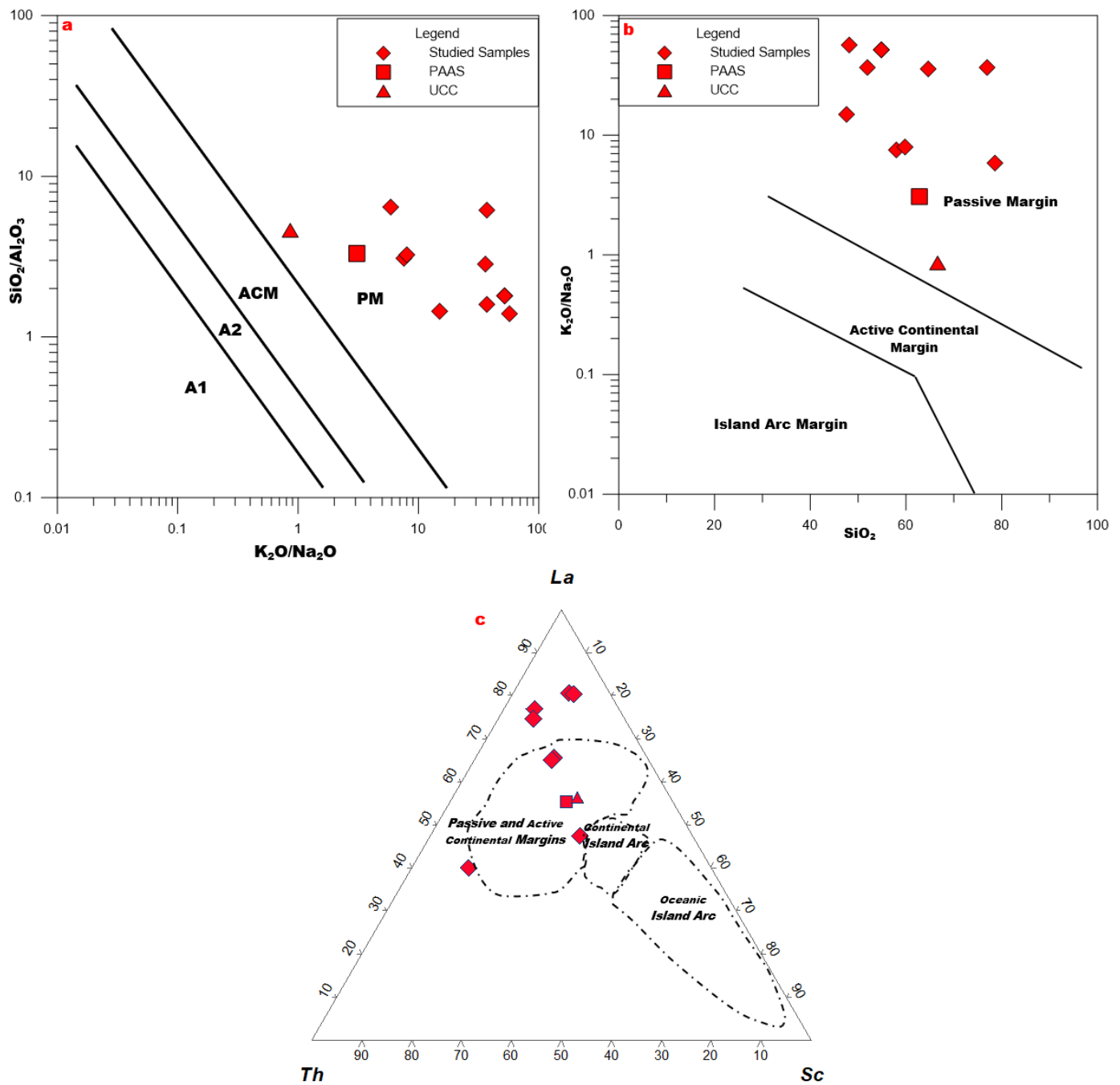


Figure 7. Discriminant; (a & b) bivariate paleotectonic plots of  $\text{SiO}_2/\text{Al}_2\text{O}_3$  versus  $\text{K}_2\text{O}/\text{Na}_2\text{O}$  after [46] and  $\log(\text{K}_2\text{O}/\text{Na}_2\text{O})$  versus  $\text{SiO}_2$  after [46] showing Passive Margin; and, (c) ternary paleotectonic plot of La-Th-Sc after [47] showing Passive Margin Settings for the studied claystone. NB: A1 – Arc setting, basaltic and andesitic detritus; A2 – Evolved arc setting, Felsic-Plutonic detritus; ACM - Active Continental Margin; PM - Passive Margin.

nance for the claystone samples. The chondrite-normalized REE pattern in Figure 6f show an overall enrichment of light rare earth elements (LREE) and depletion of heavy rare earth elements (HREE), further supporting an igneous source. For paleotectonic settings, the bivariate plots (Figures 7a-c), including  $\text{SiO}_2/\text{Al}_2\text{O}_3$  versus  $\text{K}_2\text{O}/\text{Na}_2\text{O}$ , and  $\log(\text{K}_2\text{O}/\text{Na}_2\text{O})$  versus  $\text{SiO}_2$  after Roser and Korsch [46], and La-Th-Sc after Bhatia and Crook [47], offer additional insights.

## 5.2. Weathering Indices and their relevance to sourcing industrial raw materials

Weathering indices (WI) are crucial tools in the mining and materials sourcing industries, providing insights into the composition and quality of raw materials. Therefore, application of key weathering indices (WI) in assessing the degree of alteration of claystone samples are vital in sourcing for industrial raw materials. These indices namely; the Chemical Index of Al-

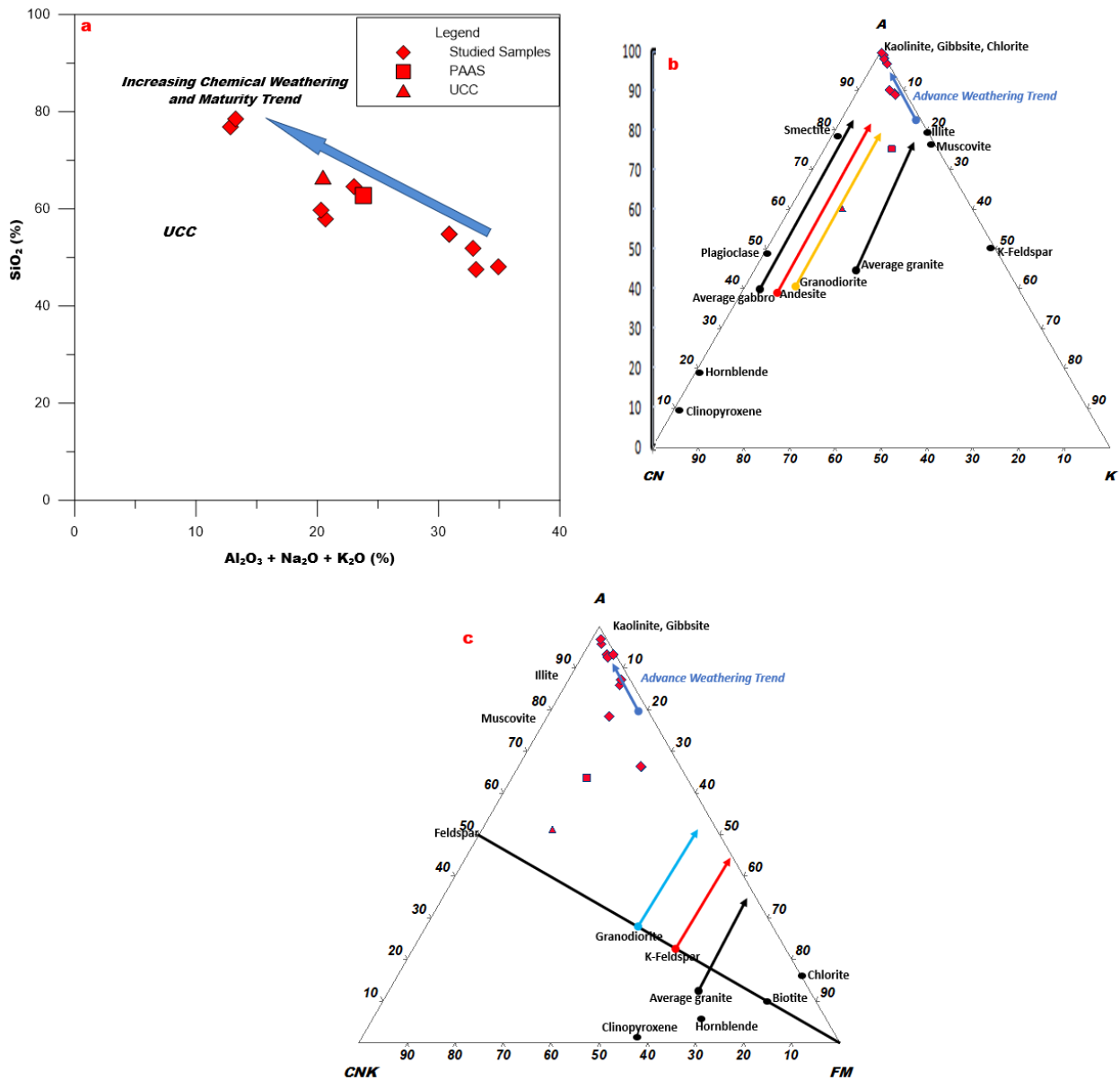


Figure 8. Discriminant bivariate chemical index plot using  $(\text{Al}_2\text{O}_3 + \text{K}_2\text{O} + \text{Na}_2\text{O})$  (%) versus  $\text{SiO}_2$  (%) after [55] showing increasing in the chemical weathering; (b & c) Discriminant ternary A-CN-K  $\{\text{Al}_2\text{O}_3 - (\text{Na}_2\text{O} + \text{CaO}) - \text{K}_2\text{O}\}$  and A-CNK-FM  $\{\text{Al}_2\text{O}_3 - (\text{CaO} + \text{Na}_2\text{O} + \text{K}_2\text{O}) - \text{Fe}_2\text{O}_3 + \text{MgO}\}$  plots after [56] showing weathering trends for the studied claystone compared with some typical source rocks.

teration (CIA), the Chemical Index of Weathering (CIW), and the Plagioclase Index of Alteration (PIA) described in previous studies by authors [48], [49], and [50], and other standard bivariate and ternary plots serve as fundamental tools for interpreting the chemical changes that occur in rocks due to weathering processes. Generally, these indices can complement each other in assessing material suitability for industrial applications and geochemical exploration, particularly in locating weathered rocks with valuable minerals.

Geochemical analysis of the studied samples revealed higher composition of  $\text{SiO}_2$  and  $\text{Al}_2\text{O}_3$ , but depletion in CaO and  $\text{TiO}_2$  (Table 1a, Figure 5a), thereby, indicating intense chemical weathering in the source area. The calculated pa-

leoweathering indices, including CIA (88.94-99.49%), CIW (96.72-99.94%), and PIA (80.40-99.03%), are consistently high (Table 1b), suggesting highly weathered claystone with potential use as raw materials in related industry. Comparison of geochemical compositions of the claystones in this study with other published data reveal Silica ( $\text{SiO}_2$ ) content above 46.5% which typically indicates presence of free quartz [51], which enhances ceramic properties. The geochemical data also aligns with standard data for paper [52], refractory bricks [53], and ceramics [54], suggesting its suitability for these applications (Table 6). While higher iron oxide ( $\text{Fe}_2\text{O}_3$ ) content could be a limitation, it may be mitigated through beneficiation, allowing for potential use. The bivariate plots of  $\text{SiO}_2$  versus  $(\text{Al}_2\text{O}_3 + \text{Na}_2\text{O} + \text{K}_2\text{O})$

[55] and the A-CN-K with A-CN-K-FM ternary diagrams [56] further confirm this trend, showing a marked increase in weathering (Figures 8a, b, & c), which points to intense weathering during formation. These findings confirm that the studied claystone is of secondary origin, and its enrichment in kaolinite, has applications in ceramics, construction, and waste management, therefore, balancing economic interests with environmental responsibility is vital for sustainable resource extraction.

## 6. Conclusions

A field-based study and sedimentological analysis of the claystone in the northern Bida Basin revealed massive and laminated claystone sub-facies, with colors ranging from white, stained-white, brown, to grey. These claystones are believed to have been deposited from suspension settling in an over-bank fines architectural element within floodplain environments. Principal Component Analysis identified two major oxides as primary contributors to the Basin, sourced mainly from weathering of surrounding Basement rocks. Geochemical proxies and plots suggested that the claystones originated from igneous source rocks and were deposited under oxic conditions. Higher paleoweathering index values (CIA, CIW, and PIA), along with A-CN-K and A-CN-K-FM ternary plots, indicated intense weathering, resulting in kaolinitic secondary clay types. These claystones are suitable as raw materials for the ceramic, paint, and chemical industries.

## Data availability

Data used in this study are available upon request from the corresponding author.

## Acknowledgement

This project was funded by the TETFUND Institutional Based Research (IBR) Grant Award 2019 through Kwara State University, Malete, Kwara State. We appreciate the Nigerian Society of Physical Science for providing the platform at the second conference of the Nigeria Society of Physical Sciences (NSPS) 2024, where this research was presented.

## References

- [1] B. Velde, "Composition and mineralogy of clay minerals", in *Origin and Mineralogy of Clays: Clays and the Environment*, Velde, B. (Ed.), Springer, Berlin, Heidelberg, 1995, pp. 8–342. <https://doi.org/10.1007/978-3-662-12648-6-2>.
- [2] H. H. Murray, "Applied Clay Science: Traditional and new applications for Kaolin, Smectite, and Palygorskite: A general overview", *Applied Clay Science* **17** (2000) 207. [https://doi.org/10.1016/S0169-1317\(00\)00016-8](https://doi.org/10.1016/S0169-1317(00)00016-8).
- [3] G. Ekosse, "X-ray powder diffraction patterns of clays and clay minerals in Botswana", Associated printers, Gaborone, Botswana, 2005, pp. 70–78. <https://search.worldcat.org/title/X-ray-powder-diffraction-patterns-of-clays-and-clay-minerals-in-Botswana/oclc/67939835>.
- [4] S. O. Onyekuru, P. O. Iwuoha, C. J. Iwuagwu, K. K. Nwozor, & K. D. Opara, "Mineralogical and geochemical properties of clay deposits in parts of Southeastern Nigeria", *International Journal of Physical Sciences* **13** (2018) 217. <https://doi.org/10.5897/IJPS2018.4733>.
- [5] D. R. Adeleye, "Cretaceous Sediments from the Shores of Lake Kainji, Nigeria", *Journal of Mining and Geology* **7** (1972) 5. [https://doi.org/10.1016/0037-0738\(74\)90013-X](https://doi.org/10.1016/0037-0738(74)90013-X).
- [6] S. P. Braide, "Syntectonic fluvial sedimentation in the central Bida Basin" *Journal of Mining and Geology* **28** (1992) 55. <https://www.sciencedirect.com/reference/108380>.
- [7] J. D. Falconer, "The Geology and Geography of Northern Nigeria," Macmillan, London (1911), pp.135-136. <https://www.sciencedirect.com/reference/119984>.
- [8] H. A. Jones, "The Oolitic ironstone of Agbaja plateau Kabba province", *Record of the Geological Survey of Nigeria*, 1958, p. 20–43. <https://www.sciencedirect.com/reference/110330>.
- [9] D. R. Adeleye, "Sedimentology of the fluvial Bida sandstones (Cretaceous), Nigeria", *Sedimentary Geology* **112** (1974) 1. [https://doi.org/10.1016/0037-0738\(74\)90013-X](https://doi.org/10.1016/0037-0738(74)90013-X).
- [10] O. Olaniyan & S. B. Olobaniyi, "Facies analysis of the Bida sandstone formation around Kajita, Nupe Basin, Nigeria", *Journal of African Earth Sciences* **23** (1996) 253. [https://doi.org/10.1016/S0899-5362\(96\)00066-8](https://doi.org/10.1016/S0899-5362(96)00066-8).
- [11] R. Olugbemiro & C. S. Nwajide, "Grain size distribution and particle morphogenesis as signatures of depositional environments of Cretaceous (Non-ferruginous) facies in the Bida Basin, Nigeria", *Journal of Mining and Geology* **33** (1997) 89.
- [12] O. J. Ojo, "Depositional environment and petrographic characteristics of Bida Formation around Share-Pategi, northern Bida Basin, Nigeria", *Journal of Geography and Geology* **4** (2012) 224. <https://doi.org/10.5539/jgg.v4n1p224>.
- [13] O. J. Ojo, & S. O. Akande, "Sedimentary facies relationships and depositional environments of the Maastrichtian Enagi Formation, northern Bida Basin, Nigeria", *Journal of Geography and Geology* **4** (2012) 136. <https://doi.org/10.5539/jgg.v4n1p136>.
- [14] S. A. Adepoju, O. J. Ojo, S. O. Akande, & B. Sreenivas "Provenance of the Campanian-Maastrichtian sandstone, northern Bida Basin: evidence from facies analysis, detrital zircon morphology and whole-rock geochemistry", *Journal of Nigerian Association of Petroleum Explorationists* **29** (2020) 59. <https://kwasuassoc.kwasu.edu.ng/items/6d57d9b3-b9f4-4673-8747-b91d1661d47a/full>.
- [15] S. A. Adepoju, O. J. Ojo, S. O. Akande, & B. Sreenivas, "Petrographic and geochemical constraints on petrofacies, provenance and tectonic setting of the Upper Cretaceous sandstones, northern Bida Basin, north-central Nigeria", *Journal of African Earth Sciences* **174** (2021) 104041. <https://doi.org/10.1016/j.jafrearsci.2020.104041>.
- [16] S. A. Adepoju, & O. J. Ojo, "Physico-chemical and mineralogical assessment of geophagy Clays from northern Bida Basin, Nigeria and their health implications", *Journal of International Medical Geologists Association-Nigeria (IMGA-Nigeria)* **16** (2022) 1. <http://dx.doi.org/10.1515/geo-2022-0507>.
- [17] M. Ghafoor, Z. Rehman, & H. A. Khan, "Enhancing claystone applications through geochemical weathering analysis", *Industrial Materials Review* **48** (2021) 478.
- [18] A. J. Whiteman, "Nigeria: Its petroleum geology, resources and potential", Graham and Trotman, London, UK, 1982, pp. 380–394. <http://dx.doi.org/10.1007/978-94-009-7361-9>.
- [19] S. B. Ojo, & D. E. Ajakaiye, "Preliminary interpretation of gravity measurements in the middle Niger Basin area, Nigeria", in *Geology of Nigeria*, C. A. Kogbe (Ed.), Elizabethan Publishing Co., Lagos, Nigeria, 1989, pp. 347-348. <https://www.scirp.org/reference/referencespapers?referenceid=1791025>.
- [20] S. B. Ojo., "Origin of a major aeromagnetic anomaly in the Middle Niger Basin, Nigeria", *Tectonophysics* **185** (1990) 162. [https://doi.org/10.1016/0040-1951\(90\)90410-A](https://doi.org/10.1016/0040-1951(90)90410-A).
- [21] J. O. Adeniyi, "Ground total magnetic intensity in parts of the Nupe Basin and the adjacent basement complex, Niger State, Nigeria", *Nigerian Journal of Applied Sciences* **3** (1985) 67.
- [22] E. E. Udensi, & I. B. Osazuwa, "Spectra determination of depths to magnetic rocks under the Nupe Basin, Nigeria", *Nigerian Association Petroleum Explorationist Bulletin* **17** (2004) 22.

- [23] D. R. Adeleye, "The Geology of the middle Niger Basin", in *Geology of Nigeria*, C. A. Kogbe (Ed.), Elizabethan Publishing Co., Lagos, 1989, p. 283.
- [24] D. R. Adeleye, "Origin of Ironstones, an Example from the Middle Niger Valley", *Journal of Sedimentary Petrology* **43** (1973) 727. <https://doi.org/10.1306/74d7284c-2b21-11d7-8648000102c1865d>.
- [25] D. R. Adeleye, & T. F. J. Dessauvagie "Stratigraphy of the Niger embayment, near Bida, Nigeria", in *African Geology*. T. F. J. Dessauvagie, & A. J. Whiteman (Eds.), University of Ibadan Press, Ibadan, 1972, p. 186.
- [26] A. D. Miall, "The Geology of fluvial deposits: sedimentary facies, Basin analysis, and petroleum geology", Springer Verlag Inc., Heidelberg, 1996, p. 582.
- [27] C. W. Rhee, W. H. Ryand, & S. K. Chough, "Contrasting development patterns of crevasse channel deposits in Cretaceous alluvial successions, Korea", *Sedimentary Geology* **85** (1993) 401. [http://dx.doi.org/10.1016/0037-0738\(93\)90095-M](http://dx.doi.org/10.1016/0037-0738(93)90095-M).
- [28] C. Reimann, P. Filzmoser, & R. G. Garrett, "Factor analysis applied to regional geochemical data: problems and possibilities", *Applied Geochemistry* **17** (2002) 185. [http://dx.doi.org/10.1016/S0883-2927\(01\)00066-X](http://dx.doi.org/10.1016/S0883-2927(01)00066-X).
- [29] T. J. Pearce, D. Wray, K. Ratcliffe, D. K. Wright, & A. Moscariello, "Chemostratigraphy of the upper Carboniferous Schooner Formation, southern North Sea", in *Carboniferous hydrocarbon geology: The southern North Sea and surrounding onshore areas*, J. D. Collinson, D. J., Evans, D. W. Holliday, & N. S. Jones (Eds.) Yorkshire Geological Society, 2005, 147–164.
- [30] J. B. Svendsen, H. Friis, H. Stollhoffen, & N. Hartley, "Facies discrimination in a mixed fluvio-eolian setting using elemental whole-rock geochemistry-Applications for reservoir characterization", *Journal of Sedimentary Research* **77** (2007) 23. <http://dx.doi.org/10.2110/jsr.2007.008>.
- [31] G. Pe-Piper, S. Triantafyllidis, & D. J. W. Piper, "Geochemical identification of clastic sediment provenance from known sources of similar geology: The Cretaceous Scotian Basin, Canada", *Journal of Sedimentary Research* **78** (2008) 595. <http://dx.doi.org/10.2110/jsr.2008.067>.
- [32] P. Filzmoser, K. Hron, & C. Reimann, "Principal component analysis for compositional data with outliers", *Environmetrics* **20** (2009) 621. <http://dx.doi.org/10.1002/env.966>.
- [33] K. Hayashi, H. Fujisawa & H. D. Holland, "Geochemistry of 1.9 Ga sedimentary rocks from northeastern Labrador, Canada", *Geochimica et Cosmochimica Acta* **61** (1997) 4115. [http://dx.doi.org/10.1016/S0016-7037\(97\)00214-7](http://dx.doi.org/10.1016/S0016-7037(97)00214-7).
- [34] M. R. Bhatia, "Plate tectonics and geochemical composition of sandstones", *Journal of Geology* **91** (1983) 611. <http://dx.doi.org/10.1086/628815>.
- [35] B. P. Roser & R. J. Korsch, "Provenance signatures of sandstone-mudstone suites determined using discrimination function analysis of major-element data", *Chemical Geology* **67** (1988) 119. [http://dx.doi.org/10.1016/0009-2541\(88\)90010-1](http://dx.doi.org/10.1016/0009-2541(88)90010-1).
- [36] K. Hayashi, H. Fujisawa & H. D. Holland, "Geochemistry of 1.9 Ga sedimentary rocks from northeastern Labrador, Canada", *Geochimica et Cosmochimica Acta* **61** (1997) 4115. [http://dx.doi.org/10.1016/S0016-7037\(97\)00214-7](http://dx.doi.org/10.1016/S0016-7037(97)00214-7).
- [37] K. C. Condie, "Chemical composition and evolution of upper continental crust: contrasting results from surface samples and shales", *Chemical Geology* **104** (1993) 1. [http://dx.doi.org/10.1016/0009-2541\(93\)90140-E](http://dx.doi.org/10.1016/0009-2541(93)90140-E).
- [38] L. Bracciali, M. Marroni, L. Pandolfi, S. Rocchi, "Geochemistry and petrography of Western Tethys Cretaceous sedimentary covers (Corsica and Northern Apennines): from source areas to configuration of margins", in *Sedimentary Provenance and Petrogenesis: Perspectives from Petrography and Geochemistry*, J. Arribas, S. Critelli, & M. J. Johnsson (Eds.), Geological Society of America Special Paper, USA, 2007, pp. 73–101. [http://dx.doi.org/10.1130/2006.2420\(06\)](http://dx.doi.org/10.1130/2006.2420(06)).
- [39] L. Zhang, D. Xiao, S. Lu, S. Jiang & S. Lu, "Effect of sedimentary environment on the formation of organic-rich marine shale: Insights from major/trace elements and shale composition", *International Journal of Coal Geology* **204** (2019) 50. <https://doi.org/10.1016/j.coal.2019.01.014>.
- [40] B. N. Nath, M. Bau, R. B. Ramalingeswara, & C. M. Rao, "Trace and rare earth elemental variation in Arabian Sea sediments through a transect across the oxygen minimum zone", *Geochimica et Cosmochimica Acta* **61** (1997) 2375. [http://dx.doi.org/10.1016/S0016-7037\(97\)00094-X](http://dx.doi.org/10.1016/S0016-7037(97)00094-X).
- [41] B. Jones, & D. C. Manning, "Comparison of geochemical indices used for the interpretation of paleo-redox conditions in ancient mudstones", *Chemical Geology* **111** (1994) 111. [http://dx.doi.org/10.1016/0009-2541\(94\)90085-X](http://dx.doi.org/10.1016/0009-2541(94)90085-X).
- [42] M. Khanebad, R. Moussavi-Harami, A. Mahboubi & M. Nadjafi "Geochemistry of carboniferous shales of the Sardar Formation, east central Iran: Implication for provenance, paleoclimate and paleo-oxygenation conditions at a passive continental margin" *Geochemistry International* **50** (2012) 867. <http://dx.doi.org/10.1134/S0016702912090029>.
- [43] S.M. Rimmer, "Geochemical Paleoredox Indicators in Devonian-Mississippian Black Shales, Central Appalachian Basin (USA)", *Chemical Geology* **206** (2004) 373. <http://dx.doi.org/10.1016/j.chemgeo.2003.12.029>.
- [44] R. L. Cullers, "Implications of elemental concentrations for provenance, redox conditions and metamorphic studies of shales and limestones near Pueblo, Co, USA. *Chemical Geology* **191** (2002) 305. [http://dx.doi.org/10.1016/S0009-2541\(02\)00133-X](http://dx.doi.org/10.1016/S0009-2541(02)00133-X).
- [45] O. J. Ojo, S. A. Adepoju, A. Awe & M. O. Adeoye, "Mineralogy and geochemistry of the sandstone facies of Campanian Lokoja formation in the Southern Bida basin, Nigeria: implications for provenance and weathering history", *Heliyon* **7** (2021) e08564. <https://doi.org/10.1016/j.heliyon.2021.e08564>.
- [46] B. P. Roser & R. J. Korsch, "Determination of tectonic Setting of Sandstone-Mudstone Suites Using SiO<sub>2</sub> Content and K<sub>2</sub>O/Na<sub>2</sub>O Ratio", *The Journal of Geology* **94** (1986) 635. <http://dx.doi.org/10.1086/629071>.
- [47] M. R. Bhatia & K. A. W. Crook, "Trace elements characteristics of graywackes and tectonic setting discrimination of sedimentary basins", *Contributions to Mineralogy and Petrology* **92** (1986) 181. <http://dx.doi.org/10.1007/BF00375292>.
- [48] H. W. Nesbitt & G. M. Young, "Early proterozoic climates and plate motions inferred from major element chemistry of lutites", *Nature* **299** (1982) 715. <http://dx.doi.org/10.1038/299715a0>.
- [49] P. Wang, Y. Du, W. Yu, T. J. Algeo, Q. Zhou, Y. Xu, L. Qi, L. Yuan, & W. Pan, "The chemical index of alteration (CIA) as a proxy for climate change during glacial-interglacial transitions in Earth history", *Earth-Science Reviews* (2020) 201. <http://dx.doi.org/10.1016/j.earscirev.2019.103032>.
- [50] K. Deng, S. Yang, & Y. Guo, "A global temperature control of silicate weathering intensity", *Nature Communications* **13** (2022) 1781. <http://dx.doi.org/10.1038/s41467-022-29415-0>.
- [51] O. A. Okunlola & O. Idowu, "Geochemistry, classification and maturity of the Eocene Nanka Formation South-East, Nigeria", *International Journal of Recent Research in Interdisciplinary Sciences (IJRRIS)* **10** (2023) 41. <https://doi.org/10.5281/zenodo.7997489>.
- [52] S. O. Onyekuru, P. O. Iwuoha, C. J. Iwuagwu, K. K. Nwozor & K. D. Opara, "Mineralogical and geochemical properties of clay deposits in parts of Southeastern Nigeria", *International Journal of Physical Sciences* **13** (2018) 217. <https://doi.org/10.5897/IJPS2018.4733>.
- [53] L. J. Suttner & P. K. Dutta, "Alluvial sandstone composition and paleoclimate Framework mineralogy", *Journal of Sedimentary Petrology* **56** (1986) 326. <http://dx.doi.org/10.1306/212F8909-2B24-11D7-8648000102C1865D>.
- [54] H. W. Nesbitt, G. M. Young, S. M. McLennan & R. R. Keays, "Effects of chemical weathering and sorting on the petrogenesis of siliciclastic sediments, with implications for provenance studies", *Journal of Geology* **104** (1996) 525. <http://dx.doi.org/10.1086/629850>.
- [55] L. J. Suttner & P. K. Dutta, "Alluvial sandstone composition and paleoclimate Framework mineralogy", *Journal of Sedimentary Petrology* **56** (1986) 326. <http://dx.doi.org/10.1306/212F8909-2B24-11D7-8648000102C1865D>.
- [56] H. W. Nesbitt, G. M. Young, S. M. McLennan & R. R. Keays, "Effects of chemical weathering and sorting on the petrogenesis of siliciclastic sediments, with implications for provenance studies", *Journal of Geology* **104** (1996) 525. <http://dx.doi.org/10.1086/629850>.